Zeitschrift: Schweizerische mineralogische und petrographische Mitteilungen = Bulletin suisse de minéralogie et pétrographie

Band: 78 (1998)

Heft: 2

Artikel: Paleoproterozoic eclogites and garnet pyroxenites of the Ubende belt (Tanzania)

Autor: Sklyarov, Eugene V. / Theunissen, Karl / Melnikov, Alexander I.

DOI: https://doi.org/10.5169/seals-59287

SCHWEIZ. MINERAL. PETROGR. MITT. 78, 257–271, 1998

Paleoproterozoic eclogites and garnet pyroxenites of the Ubende belt (Tanzania)

by *Eugene V. Sklyarov*[1], *Karl Theunissen*[2], *Alexander I. Melnikov*[1], *Jean Klerkx*[2], *Dmitry P. Gladkochub*[1] and *Abdul Mruma*[3]

Abstract

Petrographical and mineral chemical data are given for eclogites and garnet pyroxenites from the Paleoproterozoic Ubende belt which bounds the western edge of the Tanzania craton. Both types of rocks are constituents – with metaperidotites, mafic granulites, amphibolites and quartzites – of a mafic-ultramafic sequence known as Ubende and Ikulu series and interpreted as an ophiolite suite. Eclogites also occur as small lenses in garnet-kyanite gneiss. Most of the eclogites underwent strong retrogression resulting in opx-cpx coronas around garnet and in breakdown of omphacite.

Pyroxene is omphacite close to $Jd_{50}Ac_{15}Di_{35}$ in kyanite eclogite, low-Jd omphacite – Na-augite in retrograded eclogite and Na-augite to augite in garnet pyroxenites. The garnets in both eclogites and garnet pyroxenites belong to grossular-rich Prp-Alm series (Prp_{16-46}, Grs_{21-31}) with < 5 mol% spessartine. Amphibole is taramite in kyanite eclogite, edenite-pargasite in retrograded eclogites and garnet pyroxenites and pargasite in late retrogression assemblages.

The mafic-ultramafic sequence has experienced a complex metamorphic history recorded in mineral assemblages of kyanite eclogite, retrograded eclogites, mafic granulites, amphibolites, and blastomylonites. The tectonometamorphic evolution is interpreted in terms of Paleoproterozoic plate tectonics, involving a subduction of oceanic plate under the Tanzania craton and several stages of subsequent exhumation, characterized by different P-T paths.

Keywords: eclogite, garnet pyroxenite, mineral chemistry, Lower Proterozoic, Ubende belt, Tanzania craton.

Introduction

Eclogite and HP-granulites have been reported almost all around the Tanzanian craton (HEPWORTH, 1972; COOLEN, 1980). By analogy with other occurrences in Africa, e.g. Lufilian Arc (COSI et al., 1992), Dahomey (MÉNOT and SEDDOH, 1985), northern Mali (CABY, 1994) HP-metamorphism is supposed to be connected with the Upper Proterozoic Pan African orogeny. Lower Proterozoic eclogites were described in kimberlite pipes of southern Africa (e.g. SHERVAIS et al., 1988) and were found recently in the Usagara belt at the south-eastern boundary of the Tanzania craton (MÖLLER et al., 1995). Eclogites and associated garnet pyroxenites and mafic granulites were also documented in the adjacent Lower Proterozoic Ubende belt (e.g. SUTTON, 1964; HEPWORTH, 1972; SMIRNOV et al., 1973), but no detailed study of these complexes were carried out despite their significance for the metamorphic and tectonic evolution of the Ubende belt in particular and for plate tectonic processes during Lower Proterozoic orogeny.

This paper describes occurrences, mineral assemblages, mineral chemistry, and the P-T evolution of eclogites and garnet amphibolites of the Ubende belt. It presents a first attempt to interpret the presence of these HP-metamorphic rocks in the tectonic evolution of the belt.

Geologic setting

The north-west trending Ubende belt extends for over 500 km to the western side of the Tanzania

[1] Institute of the Earth's Crust RAS, Lermontova St. 128, 664033 Irkutsk, Russia. <skl@gpg.crust.irk.ru>
[2] Royal Museum of Central Africa, Department of Geology and Mineralogy, 3080 Tervuren, Belgium.
[3] University of Dar es Salaam, Department of Geology, P.O. Box 35091, Dar es Salaam, Tanzania.

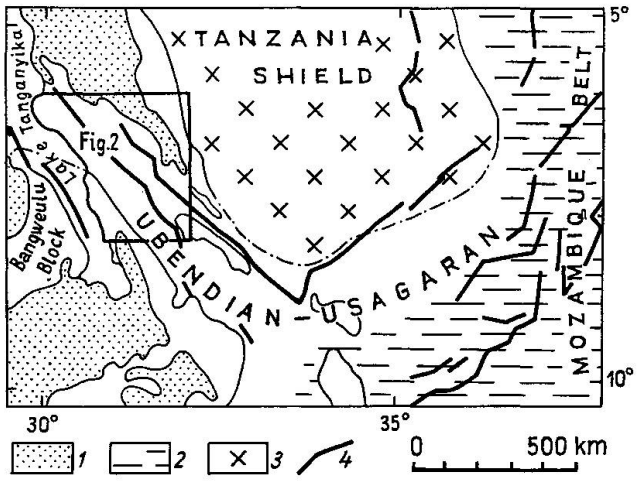

Fig. 1 Sketch map, showing position of the Ubende belt in the regional structure (modified after PRIEM et al., 1979).
1 – Upper Proterozoic deposits; 2 – Pan-African thermal effect on Lower Proterozoic belts; 3 – Tanzanian shield; 4 – major recent faults. Contour of figure 2 is shown.

craton (Fig. 1). It is about 150 km wide and limited to the north by the NE–SW striking Middle Proterozoic Kibara belt and the Neoproterozoic Bukoban sedimentary basin, to the west by the Lower Proterozoic Bangweulu Block (DALY and UNRIG, 1982). Based on a large scale kinematic approach the Ubende- and Usagara fold belts have been interpreted by DALY et al. (1985) as originating within a single Paleoproterozoic plate tectonic regime, i.e. the EW and NE oriented Usagara thrust belt (SHACKELTON and RIES, 1984) which results from frontal accretion on the Archean craton, while the NW oriented Ubende shear belt was interpreted as a result of lateral accretion.

The Ubende belt is composed of blocks or terranes which are strongly elongated in a NW–SE direction and which are bounded by shear zones (DALY, 1988; DALY et al., 1989). In the central part six main series are distinguished (Fig. 2):

– the Mahali series consisting mainly of two-mica quartz-feldspatic gneisses exhibiting widespread granitization;

– the Ufipa series also composed of granitic gneisses but with a higher proportion of amphibole-bearing gneisses, containing pods of hornblendite and retrograded eclogite;

– the Katuma series notable for a homogeneous lithology of biotite-plagioclase gneisses and granite-gneisses, commonly migmatised;

– the Ikulu series composed of amphibolites with lenses of harzburgite, pyroxenite, garnet pyroxenites, eclogites, retrograded eclogites, high-P granulites and quartzites of different size;

– the Ubende series characterized essentially by amphibolite and amphibole gneisses with lenses of listwenite, pyroxenite, hornblendite, and high-P granulite of different size;

– the Wansisi series which is mainly composed of aluminoferrous gneisses, sometimes associated with amphibolites and Fe–Mn quartzites and with rare boudins of hornblendite and retrograded granulite in gneisses.

The Ubende and Ikulu series are essentially composed of rocks of mafic composition and may be regarded as equivalents. The main difference between both series is the different degree of overprint of the early eclogite- and granulite-facies assemblages by regional widespread deformation and retrogression to amphibolite facies. In the Ikulu series the proportion of the early mafic granulites and pyroxenites is much higher than in the Ubende series.

Fragments of metamorphosed harzburgite, pyroxenites, gabbro, eclogite and mafic granulite (former basalts or diabase dikes) and Fe–Mn quartzite (metacherts) embedded in amphibolites and amphibole gneisses are supposed to represent relics of an original ophiolite suite.

Recent investigation of the Ubende belt provides a good insight in its structural development. Roughly two different Paleoproterozoic evolutionary phases were proposed (THEUNISSEN et al., 1996). Although time constraints are only partly

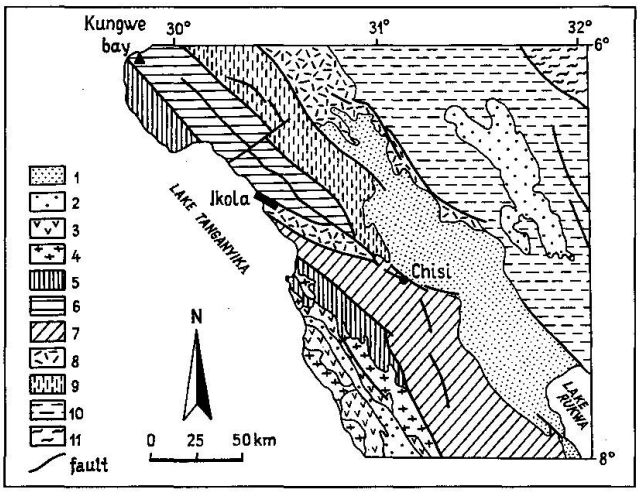

Fig. 2 The Ubendian terranes along lake Tanganyika.
1 – recent deposits; 2 – Upper and Middle Proterozoic horizontal deposits; 3 – Lower Proterozoic volcanics; 4 – Lower Proterozoic granites. Ubendian terranes: 5 – Mahali series; 6 – Ubende series; 7 – Ufipa series; 8 – Ikulu series; 9 – Wansisi series; 10 – Katuma series. 11 – Dodomian series (Tanzanian shield). Location occurrence of garnet pyroxenites (solid triangle), retrograded eclogites (solid circle) and kyanite eclogite, retrograded eclogites and garnet pyroxenites (solid square) are shown.

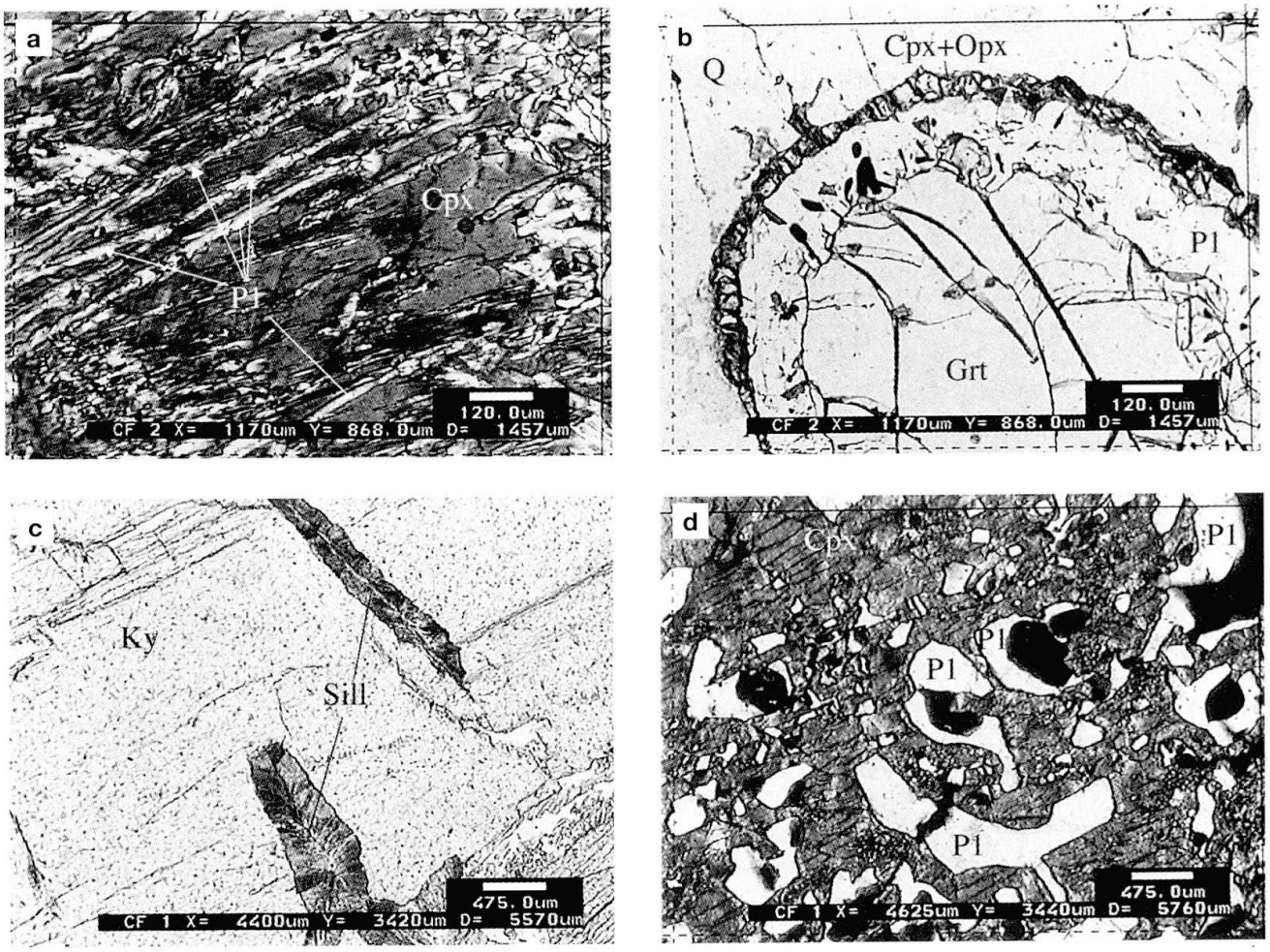

Fig. 3 Photomicrographs showing mineral associations and texture of eclogites from the Ubende belt. (a) Exsolution lamellae of plagioclase in Na-augite in retrograded eclogite (sample Sk-1 from Ikola area). Composition of Cpx is listed in table 2. (b) Corona around garnet in contact with quartz in retrograded eclogite (sample Sk-1 from Ikola area). Internal part of the corona is composed of plagioclase with rare grains of opaque mineral and amphibole. External part consists of orthopyroxene and clinopyroxene. Composition of garnet, orthopyroxene and clinopyroxene listed in tables 1 and 2. (c) Large grain of kyanite in kyanite eclogite. Aggregate of sillimanite along joints corresponds to near isothermal decompression trend of late exhumation stage (sample TZS1 from Ikola area). Composition of associated minerals are listed in tables 1, 2, 3. (d) Sieve-textured Al-rich Na-augite with inclusions of sodic plagioclase (light) and amphibole (dark) in retrograded eclogite (sample 279a2 from Chisi area). Composition of pyroxene is listed in table 2.

documented, it was proposed that an early evolutionary stage with granulite facies environment occurred during the 2100–2025 Ma period, while a second phase with amphibolite facies conditions and NW oriented folding and shearing took place between 1950 and 1850 Ma, ending with the late-tectonic magmatism (LENOIR et al., 1994). It is important to note that available geochronological data (LENOIR et al., 1994; BOVEN et al., 1996) confirm that, despite subsequent structural reactivation, no major orogen scale impact affected the Ubende belt after 1720–1740 Ma.

Fragments of eclogites and garnet pyroxenites as well as mafic granulites and garnet-free ultramafics were investigated in the Ikola, Kungwe Bay and Chisi areas (see Fig. 2). Although the structural relations with embedding amphibolites and amphibolite gneiss are not always visible, the transition of massive retrograded eclogite to foliated plagioclase-poor garnet amphibolite, to plagioclase-rich garnet amphibolite and to garnet-free amphibolite was documented. Many pods are massive and relatively homogenous; some are compositionally layered. The size of the lenses varies from tens of centimeters to tens of meters across in the Ikola and Kungwe Bay areas and from tens of centimeters to a few meters across in the Chisi area.

Petrography

According to mineral content and mineral chemistry plagioclase-free garnetiferous rocks can be subdivided into four groups: kyanite eclogite, retrograded eclogites, amphibole-bearing garnet clinopyroxenites and amphibole-bearing garnet websterite. It should be noted that the above mentioned varieties occur in different outcrops and that transitions from fresh to retrograded eclogite or from retrograded eclogite to mafic granulite were never observed.

(1) *Kyanite eclogite* occurs as isolated body in garnet amphibolites. The rock is coarse-grained showing a granoblastic heterogranular texture and slight foliation, defined by subparallel oriented grains of omphacite, taramite and sodic plagioclase. The mineral assemblages of the eclogite may be subdivided into several groups in sequential order of formation:

(a) garnet-omphacite-taramite-kyanite-sodic plagioclase-quartz-rutile. Garnets occur as porphyroblasts (up to 1 cm) embedded in a polygonal equigranular cpx-amf-pl matrix. Inclusions of omphacite, taramite and rutile are usual. Subhedral omphacite and taramite in the matrix range from 1 to 3 mm across. Sodic plagioclase, being in equilibrium with omphacite and taramite, is usually concentrated in microlayers (1–2 mm thick). Relatively rare porphyroblastic prismatic grains of kyanite occur in the matrix. Rutile is ubiquitous, either as interstitial grains between rock-forming minerals or as fine-grained inclusions in garnet or omphacite. Ilmenite occurs in aggregates with rulile in matrix.

(b) sillimanite, which develops along cracks in kyanite (Fig. 3c) and fixes the stage of high temperature retrogression;

(c) zoisite, developing as euhedral oriented grains in matrix. Growth of zoisite seems to postdate all the other primary minerals, corresponding to late lower temperature retrogression.

(2) *Retrograded eclogites* are identified by the presence of relics of omphacite, textures of primary pyroxene breakdown (lamellae of sodic plagioclase (Fig. 3a) or sieve-textured grains of pyroxenes (Fig. 3d). In the Ikola and Kungwe Bay areas they are medium- to coarse-grained, mostly massive with near-equigranular texture, but sometimes exhibiting a foliation defined by alternation of garnet-rich and garnet-poor layers. The former mineral constituents are garnet, pyroxene 1, green amphibole, rutile, whereas pyroxene 2, blue-green amphibole, plagioclase, scapolite and titanite reflect the stage of high-temperature retrogression. Sometimes high-temperature retrogression is characterized by development of coronas around garnet in contact with quartz (Fig. 3b). The inner part of a corona is composed of plagioclase with rare grains of green amphibole, while the outer part contains an opx-cpx assemblage.

Retrograded eclogites of the Chisi area are medium-grained, massive equigranular and relatively rich in plagioclase and quartz (up to 20–30%). The sieve-textured intergrowth of Na-augite, plagioclase and amphibole is supposed to be the coarse scale analogue of symplectites, usual in retrograded eclogites. The coarseness of the sieve texture relative to normal symplectites presumably reflects unusually high temperatures, or longer period of plagioclase and amphibole release, or both (SANDERS et al., 1987). The early eclogite stage is supported by the relics of omphacite in the core of some pyroxene grains.

(3) *Garnet pyroxenites* are more abundant than the two previous groups of rocks and may be subdivided into two subgroups according to textural features. Coarse-grained varieties are composed mostly of garnet and pyroxene with minor amphibole. The only distinction between the true eclogites and garnet clinopyroxenites is that clinopyroxenes contain less Na (Fig. 6) and are not omphacite. The lower Na content in the pyroxenes probably reflects a bulk rock composition low in Na, since modal mineral contents and the extent of retrogression are similar.

(4) *Garnet websterites* occur sporadically among garnet-free websterites, which compose large blocks of 50–60 m thickness in amphibolites. They are heterogranular, massive, medium- to coarse-grained rocks. Fine-grained garnet develops along the margins of subhedral pyroxene grains.

All the rocks described contain disequilibrium texture and phases related to granulite- to amphibolite-facies decompression. Retrogressive amphibolitization is manifested as later, fine-grained, texturally immature blue-green hornblende along fractures. It is worth noting that amphibole-filled fractures develop only in pods of retrograded eclogites, garnet pyroxenites and mafic granulites, and have never been observed in embedding amphibolites.

Mineral chemistry

Mineral analyses were carried out on a CAMECA microprobe at the Buryat Geological Institute, Ulan-Ude. Standard operating conditions were 15 kV, 20 nA; various natural standards were used in calibration. The Fe^{3+} and Fe^{2+} contents in minerals were calculated using the method of DROOP (1987).

Tab. 1 Representative analyses of garnets. Abbreviations: c – core, r – rim, Ky-ecl – kyanite eclogite, R-ecl – retrograded eclogite, Grt-px – garnet pyroxenite, Grt-wb – garnet websterite. Formula calculations after DROOP (1987).

Sample	TZS-1	TZS-1	Sk-1	Sk-1	Sk35e	279a2	Sk82h	n24b	n24b	Sk42a	Sk55e
Rock	Ky-ecl	Ky-ecl	R-ecl	R-ecl	R-ecl	R-ecl	R-ecl	Grt-px	Grt-px	Grt-px	Grt-wb
Min	c	r	c	r	r	r	r	c	r	c	c
Area	Ikola	Ikola	Ikola	Ikola	Ikola	Chisi	Chisi	Ikola	Ikola	Ikola	Ikola
SiO_2	38.37	38.32	39.38	38.67	39.63	38.91	38.22	39.88	40.05	39.09	39.94
Al_2O_3	21.33	21.57	22.18	21.92	21.04	21.84	21.21	22.33	22.45	21.72	22.17
Cr_2O_3	0.00	0.07	0.00	0.00	0.06	0.00	0.00	0.14	0.14	0.08	0.15
FeO_{tot}	26.20	23.17	21.94	22.87	24.80	23.07	25.87	19.07	20.16	19.62	19.61
MnO	1.39	0.81	0.61	0.95	0.96	0.53	0.56	0.38	0.48	0.15	0.52
MgO	4.07	6.00	9.15	7.13	5.00	7.13	5.72	11.14	10.69	7.09	11.63
CaO	8.94	9.54	6.74	7.50	9.51	7.83	7.57	6.84	6.26	11.31	6.20
Total	100.35	100.03	100.05	99.04	100.07	99.31	99.21	99.78	100.23	99.07	99.72
8 cations; 12 oxygens											
Si	3.002	3.000	2.993	3.000	3.008	3.009	2.997	2.995	3.006	3.006	3.001
Al	1.968	1.965	1.988	2.005	1.971	1.991	1.960	1.977	1.986	1.969	1.964
Cr	0.000	0.004	0.000	0.000	0.004	0.000	0.000	0.008	0.008	0.005	0.009
Fe^{3+}	0.028	0.031	0.026	0.000	0.039	0.000	0.036	0.025	0.000	0.006	0.026
Fe^{2+}	1.686	1.466	1.369	1.484	1.576	1.492	1.660	1.173	1.266	1.256	1.177
Mn	0.092	0.053	0.039	0.062	0.063	0.035	0.037	0.024	0.031	0.010	0.033
Mg	0.475	0.691	1.037	0.824	0.580	0.822	0.667	1.247	1.196	0.813	1.291
Ca	0.749	0.790	0.549	0.623	0.793	0.649	0.636	0.550	0.503	0.932	0.499
Total	8.000	8.000	8.000	7.998	8.000	7.996	8.000	8.000	7.997	8.000	8.000
X_{Fe}	0.562	0.489	0.457	0.496	0.523	0.498	0.553	0.392	0.423	0.417	0.392
X_{Mn}	0.031	0.018	0.013	0.021	0.021	0.012	0.012	0.080	0.010	0.003	0.011
X_{Mg}	0.158	0.230	0.346	0.275	0.193	0.274	0.223	0.416	0.399	0.270	0.430
X_{Ca}	0.250	0.263	0.183	0.208	0.263	0.216	0.262	0.184	0.168	0.310	0.167

Tab. 2 Representative analyses of pyroxenes. Abbreviations: c – core, cr – in corona, i – inclusion in garnet, m – in matrix, r – rim, rl – relics in the central part of the grain. Other abbreviations as in table 1. Formula calculations after DROOP (1987).

Sample	TZS-1	TZS-1	TZS-1	Sk-1	Sk-1	Sk-1	Sk35e	Sk35e	n24b	n24b
Rock	Ky-ecl	Ky-ecl	Ky-ecl	R-ecl	R-ecl	R-ecl	R-ecl	R-ecl	Gr-px	Gr-px
Min	Cpx m	Cpx ic	Cpx ir	Cpx m	Cpx cr	Opx cr	Cpx rl	Cpx r	Cpx c	Cpx r
Area	Ikola	Ikola	Ikola	Ikola	Ikola	Ikola	Ikola	Ikola	Ikola	Ikola
SiO_2	53.59	53.25	54.02	51.32	52.05	51.97	53.57	52.71	52.46	52.49
TiO_2	0.30	0.08	0.09	0.46	0.00	0.00	0.32	0.44	0.35	0.28
Al_2O_3	14.41	12.76	14.28	5.11	1.82	0.56	7.95	4.49	6.91	6.76
Cr_2O_3	0.00	0.07	0.07	0.06	0.05	0.06	0.00	0.00	0.11	0.00
FeO_{tot}	6.77	11.77	10.80	8.36	9.06	24.89	7.98	9.26	5.31	5.21
MnO	0.00	0.12	0.12	0.14	0.21	0.37	0.05	0.03	0.00	0.00
MgO	5.35	3.51	3.29	12.91	12.93	20.75	8.85	10.31	12.6	13.07
CaO	9.31	8.55	7.60	19.96	21.77	0.44	16.91	20.17	18.63	19.16
Na_2O	8.70	8.49	9.22	1.71	0.95	0.00	4.76	2.25	2.98	2.56
K_2O	0.00	0.00	0.00	0.00	0.00	0.00	0.00	0.05	0.00	0.00
Total	98.43	99.13	100.0	100.39	99.10	99.04	99.92	99.78	99.35	99.53
			4 cations		6 oxygens					4 cations
Si	1.927	1.950	1.946	1.887	1.956	1.976	1.954	1.961	1.909	1.909
Ti	0.008	0.002	0.002	0.013	0.000	0.000	0.009	0.012	0.010	0.008
Al	0.611	0.551	0.606	0.221	0.081	0.025	0.342	0.197	0.296	0.290
Cr	0.000	0.002	0.002	0.002	0.001	0.002	0.000	0.000	0.003	0.000
Fe^{3+}	0.126	0.145	0.139	0.099	0.075	0.021	0.069	0.021	0.073	0.058
Fe^{2+}	0.078	0.216	0.187	0.158	0.210	0.770	0.174	0.267	0.089	0.101
Mn	0.000	0.004	0.004	0.004	0.007	0.012	0.002	0.001	0.000	0.000
Mg	0.287	0.192	0.177	0.707	0.724	1.176	0.481	0.572	0.684	0.709
Ca	0.359	0.336	0.293	0.786	0.877	0.018	0.633	0.804	0.726	0.747
Na	0.606	0.603	0.644	0.122	0.069	0.000	0.337	0.162	0.210	0.180
K	0.000	0.000	0.000	0.000	0.000	0.000	0.000	0.002	0.000	0.000
Total	4.000	4.000	4.000	4.000	4.000	4.000	4.000	4.000	4.000	4.000
Mol%Jd	48.0	45.8	50.5	2.3	0.0		26.7	14.2	13.7	12.2
Mol%Ac	12.6	14.5	13.9	9.9	7.0		6.9	2.1	7.3	5.8
Mol%Aug	39.4	39.7	35.6	87.8	93.1		66.3	83.8	79.0	82.0

Representative analyses of minerals are presented in tables 1–3, compositional variations are shown in figures 4–6 and characteristic features of the mineral chemistry are described below.

GARNET

The composition of the analyzed garnets with respect to the mole proportions of Mg, Fe, Mn and Ca are presented in figure 4. The garnets in both eclogites belong to a grossular-rich prp-alm series with < 5 mol% spessartine. They show a relatively wide range of pyrope contents (16–46 mol%) with little variation in grossular component (21–31 mol%). Two groups of garnets are distinguished in garnet pyroxenites (Fig. 4). The first group is similar to garnets of retrograded eclogites, though slightly richer in grossular component. Garnets of the second group are pyrope-rich (39–46 mol%), reflecting probably a bulk composition rich in MgO. In general the analysed garnets show only weak effects of retrograde evolution, as reflected by weakly decreasing MgO from core to rim. Only in garnets from kyanite eclogite the prograde trend is preserved as shown on figure 5a.

CLINOPYROXENES

The composition ranges of clinopyroxene are shown on an augite-jadeite-acmite diagram (Fig. 6). Three groups can be chemically distinguished

Tab. 2 (cont.)

Sample	Sk42a	Sk55e	Sk55e	279a2	279a2	Sk82h	Sk82h	Sk82h	Sk82k	Sk8f	Sk8f
Rock	Gr-px	Gr-wb	Gr-wb	R-ecl	R-ecl	R-ecl	R-ecl	R-ecl	R-ecl	Gr-wb	Gr-wb
Min	Cpx r	Cpx r	Opx r	Cpx c	Cpx r	Cpx i	Cpx rl	Cpx r	Cpx r	Opx	Cpx
Area	Ikola	Ikola	Ikola	Chisi	Chisi	Chisi	Chisi	Chisi	Chisi	Kungwe	Kungwe
SiO_2	51.02	52.38	53.94	52.71	52.64	52.55	52.14	52.31	51.66	54.03	52.21
TiO_2	0.59	0.34	0.06	0.30	0.34	0.48	0.43	0.32	0.32	0.00	0.21
Al_2O_3	5.57	3.90	2.59	7.38	7.15	6.73	8.56	3.60	6.56	3.22	5.08
Cr_2O_3	0.08	0.23	0.10	0.10	0.11	0.00	0.05	0.00	0.00	0.00	0.00
FeO_{tot}	5.10	4.64	13.63	8.16	8.34	9.04	9.96	9.82	7.43	12.37	6.55
MnO	0.00	0.05	0.11	0.05	0.05	0.08	0.08	0.10	0.09	0.00	0.00
MgO	12.87	13.85	28.34	10.01	10.00	9.73	8.41	11.82	10.23	30.55	12.49
CaO	22.94	23.18	0.24	17.68	17.65	16.39	15.82	20.76	20.73	0.00	21.05
Na_2O	0.89	0.87	0.00	3.44	3.17	3.74	4.24	1.15	2.18	0.00	2.08
K_2O	0.00	0.00	0.00	0.00	0.00	0.03	0.00	0.00	0.00	0.00	0.00
Total	99.06	99.46	99.01	99.98	99.48	98.95	99.94	99.89	99.24	100.17	99.67
		6 oxygens			4 cations			6 oxygens			
Si	1.892	1.931	1.942	1.932	1.943	1.949	1.919	1.952	1.920	1.901	1.915
Ti	0.016	0.009	0.002	0.008	0.009	0.013	0.012	0.009	0.009	0.000	0.006
Al	0.244	0.169	0.110	0.319	0.311	0.294	0.371	0.158	0.287	0.133	0.220
Cr	0.002	0.007	0.003	0.003	0.003	0.000	0.001	0.000	0.000	0.000	0.000
Fe^{3+}	0.000	0.005	0.000	0.042	0.008	0.050	0.068	0.002	0.011	0.065	0.086
Fe^{2+}	0.158	0.138	0.410	0.209	0.249	0.230	0.238	0.304	0.220	0.299	0.115
Mn	0.000	0.002	0.003	0.002	0.002	0.003	0.002	0.003	0.003	0.000	0.000
Mg	0.711	0.761	1.521	0.547	0.550	0.538	0.461	0.657	0.567	1.602	0.683
Ca	0.912	0.916	0.009	0.694	0.698	0.652	0.624	0.830	0.826	0.000	0.827
Na	0.064	0.062	0.000	0.245	0.227	0.269	0.303	0.083	0.157	0.000	0.148
K	0.000	0.000	0.000	0.000	0.000	0.001	0.000	0.000	0.000	0.000	0.000
Total	4.000	4.000	4.000	4.000	4.000	4.000	4.000	4.000	4.000	4.000	4.000
Mol%Jd	6,4	5,7		20.3	21.8	21.9	23.4	8.1	14.6		6.2
Mol%Ac	0,7	0,6		4.2	0.8	5.0	6.8	0.2	1.1		8.6
Mol%Aug	92,7	93,8		75.5	77.3	73.1	69.7	91.7	84.3		85.2

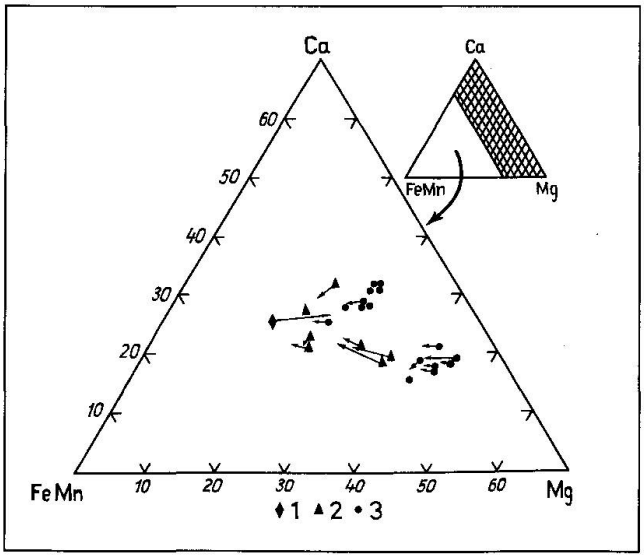

as Jd-rich omphacite, Jd-poor omphacite – Al rich Na-augite and Na-augite – augite.

Omphacite (Jd-content up to 50%) occurs only in kyanite eclogite and either as grains in the matrix or as inclusions in garnets. The pyroxenes in both sites have similar Jd-content but the pyroxene in the matrix is richer in MgO. This is in good correlation with the decrease of Mg/Mg + Fe from core to rim in the garnet. The pyroxene inclusions in the garnets show a prograde trend, or increase Jd-content from core to rim (Fig. 5b), whereas pyroxenes in the matrix show decrease of

Fig. 4 Mole proportions of Ca–Fe–Mg for garnets from: 1 – kyanite eclogite, 2 – retrograded eclogites, 3 – garnet pyroxenites. Arrows represent change of composition from core to rim.

Tab. 3 Representative analyses of amphiboles. Abbreviations as in table 1. Formula calculations after DROOP (1987).

Sample	TZS-1	TZS-1	Sk35e	Sk35f	n24b	Sk42a	Sk55e	Sk37d	279a2	Sk82h	Sk82k	Sk8f
Rock	Ky-ecl	Ky-ecl	R-ecl	R-ecl	Grt-px	Grt-px	Grt-wb	R-ecl	R-ecl	R-ecl	R-ecl	Grt-wb
Min	i	m										
Area	Ikola	Ikola	Ikola	Ikola	Ikola	Ikola	Ikola	Ikola	Chisi	Chisi	Chisi	Kungwe
SiO_2	37.88	41.14	43.89	38.97	44.80	44.13	44.67	43.14	41.61	43.04	46.03	44.34
TiO_2	0.00	0.49	0.51	0.12	0.95	1.11	1.29	1.44	1.39	1.44	0.58	1.22
Al_2O_3	18.67	14.97	12.49	19.73	13.35	14.05	12.06	14.36	14.33	12.48	9.60	12.39
Cr_2O_3	0.00	0.00	0.06	0.11	0.00	0.09	0.57	0.00	0.07	0.06	0.00	0.20
FeO_{tot}	19.84	16.42	14.53	12.02	7.33	9.11	6.80	10.23	14.05	16.14	12.93	9.33
MnO	0.40	0.00	0.06	0.08	0.00	0.00	0.03	0.00	0.00	0.08	0.06	0.00
MgO	5.97	10.13	11.05	11.00	17.22	13.62	15.75	13.15	11.76	9.71	12.88	15.07
CaO	6.90	10.13	11.94	11.29	11.32	12.25	12.41	12.83	11.25	11.17	11.80	11.49
Na_2O	6.08	4.23	2.44	3.10	2.54	1.89	1.69	1.99	2.32	2.26	1.73	2.11
K_2O	0.57	0.00	0.38	0.19	0.00	0.15	1.17	0.37	0.42	0.76	0.12	1.63
Total	96.31	97.51	97.46	97.26	97.51	96.54	96.49	97.54	97.20	97.33	96.00	99.78
23 oxygen cations; cations – (Ca + Na + K) = 13.000												
Si	5.748	6.080	6.505	5.698	6.280	6.409	6.489	6.280	6.086	6.437	6.813	6.385
Ti	0.000	0.054	0.057	0.013	0.100	0.121	0.141	0.158	0.153	0.162	0.065	0.132
Al	3.339	2.607	2.182	3.400	2.205	2.405	2.065	2.464	2.471	2.200	1.675	2.103
Cr	0.000	0.000	0.007	0.013	0.000	0.010	0.065	0.000	0.008	0.007	0.000	0.023
Fe^{3+}	1.009	0.698	0.122	0.714	0.000	0.151	0.053	0.028	0.780	0.213	0.307	0.405
Fe^{2+}	1.508	1.332	1.679	0.756	0.859	0.955	0.773	1.218	0.938	1.806	1.294	0.719
Mn	0.051	0.000	0.008	0.010	0.000	0.000	0.004	0.000	0.000	0.010	0.008	0.000
Mg	1.350	2.232	2.441	2.397	3.598	2.948	3.410	2.853	2.564	2.164	2.839	3.235
Ca	1.122	1.604	1.896	1.769	1.700	1.906	1.932	2.001	1.763	1.790	1.872	1.773
Na	1.789	1.212	0.701	0.879	0.690	0.532	0.476	0.562	0.658	0.655	0.497	0.589
K	0.110	0.000	0.072	0.035	0.000	0.028	0.217	0.069	0.078	0.145	0.023	0.299
Total	16.027	15.819	15.669	15.683	15.433	15.466	15.625	15.632	15.500	15.591	15.391	15.662

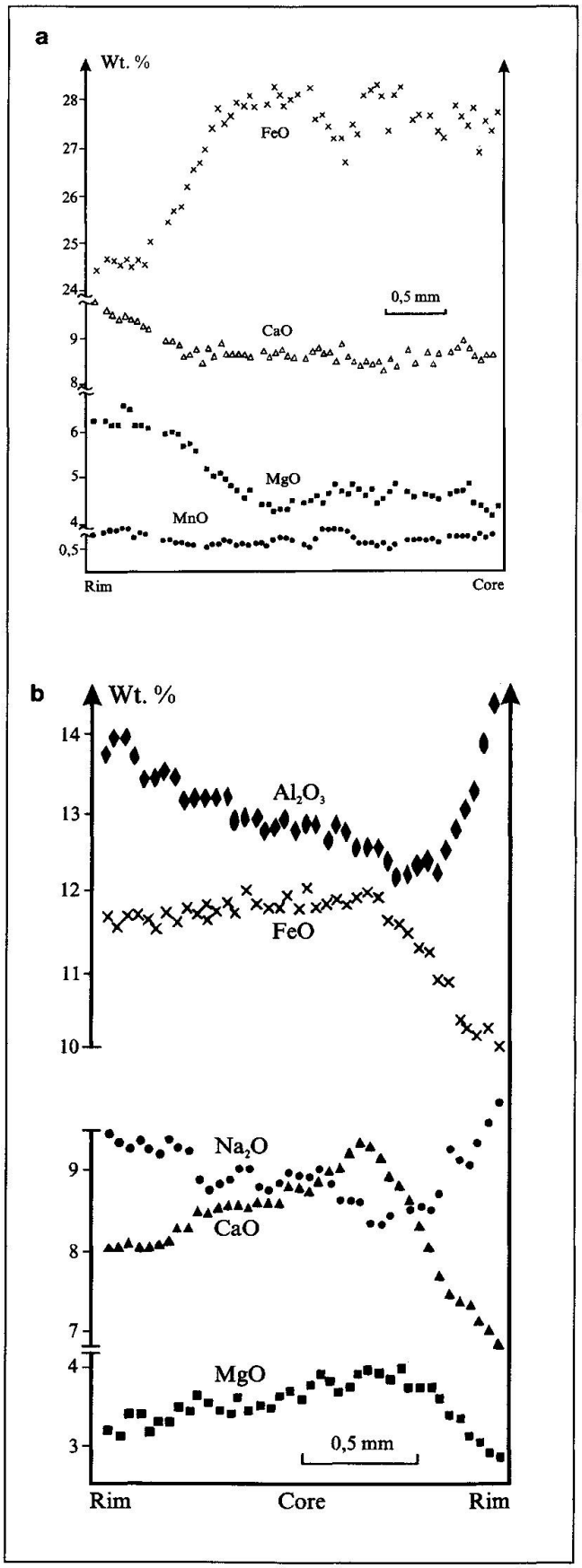

Fig. 5 Compositional profiles for (a) garnet and (b) pyroxene inclusion in garnet. Kyanite eclogite, sample TZS1.

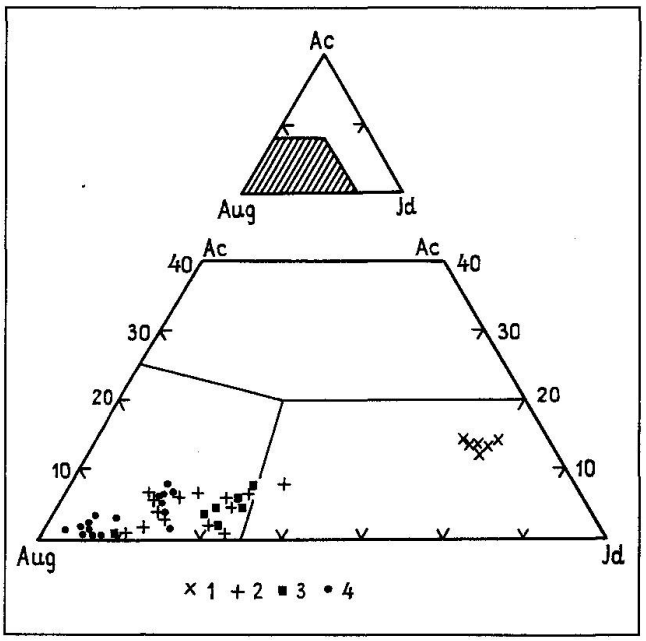

Fig. 6 Compositional variations of clinopyroxenes from eclogites and garnet pyroxenites. 1 – kyanite eclogite; 2 – retrograded eclogites (Ikola); 3 – retrograded eclogites (Chisi); 4 – garnet pyroxenites (Ikola and Kungwe bay areas).

jadeite in rims. The calculated acmite content is relatively high and constant (13–14%). Low-Jd omphacite and Na-augite occur as relics in the central parts of pyroxene grains of retrograded eclogites. Na-augite and augite are the most common pyroxenes in retrograded eclogites and garnet pyroxenites.

Na-augite in retrograded eclogite contains 6–15% of the jd component. In rocks with a high temperature retrograde overprint, two types of clinopyroxene are distinguished; the matrix pyroxene has a 15% Jd content while in the cpx-opx-pl coronas around garnet (Fig. 3b) the pyroxene is almost jadeite-free. In view of the exsolution lamellae of plagioclase in pyroxene (Fig. 3a) it is suggested that omphacite was the primary pyroxene .

AMPHIBOLE

In the analysed amphiboles (Tab. 3) three compositional groups may be distinguished as taramite, edenite-pargasite and pargasite.

Alumino-taramite $NaCaNa(Mg,Fe^{2+})_3Al_2Si_6Al_2O_{22}(OH)_2$ appears in kyanite eclogite, where it occurs in the groundmass and in inclusions in garnet. Taramite, first identified by UNGARETTI (et al., 1981) is indicative for relatively high-temperature (CHOPIN and SOBOLEV, 1995) and high-pressure metamorphic conditions. In inclusions in garnet,

taramite has a much higher content of alkalies and a lower Mg/Mg + Fe ratio than taramite in the groundmass. The groundmass taramite is transitional between alumino-taramite and alumino-barroisite $CaNa(Mg,Fe^{2+})_3(Fe^{3+},Al)_2Si_7AlO_{22}(OH)_2$.

Most common amphiboles of the edenite-pargasite group occur in all rock-types under consideration. Usually their composition is only weakly variable from core to rim but in some cases a sharp increase of Al_2O_3 and alkali appears in the rim zone.

Pargasite, replacing former minerals and developed along fractures narrow veins has high Al_2O_3 (up to 19%) and alkali content and also higher Fe/Fe + Mg ratio than coexisting former amphiboles.

OTHER MINERALS

Sodic plagioclase, whose content in the retrograded eclogites and some garnet pyroxenites does not exceed 1–2%, ranges in composition from An_6 to An_{30}, rarely up to An_{50}. Compositions of analyzed scapolites mostly range between Me_{66} and Me_{73}, with mizzonite (Me_{44}) in one sample of retrograded eclogite (Sk-1). The MgO content in ilmenite of kyanite eclogites reaches 1.5%, but is insignificant in retrograded eclogites and associated mafic granulites.

Geothermobarometry

Estimation of the P-T conditions of crystallization of eclogites and garnet pyroxenites is a complex problem because an individual sample usually contains disequilibrium assemblages reflecting different stages of evolution.

Many geothermometers and geobarometers are applicable to the mineral assemblages present in the studied rocks. Two complementary approaches were applied to the rocks of the Ubende belt. At first temperatures were determined from the Fe–Mg exchange reaction between garnet and clinopyroxene (ELLIS and GREEN, 1979) with Fe^{3+} being recalculated for both minerals. Both retrograded eclogites and garnet pyroxenites give a wide range of temperatures from 700 to 850 °C. The temperatures obtained using core compositions of analyzed minerals are systematically 20–50 °C higher than for rim compositions.

Geobarometry is notoriously difficult to determine in Pl-free assemblages, and only minimum pressures between 10 and 14 kbar could be established for retrograded eclogites and garnet pyroxenites from the albite = jadeite + quartz reaction (HOLLAND, 1980). For retrograded eclogite (279a2), where omphacite is proposed to be in equilibrium with sodic plagioclase, more precise P-estimations of about 14 kbar were obtained, by using equilibration P with T in garnet-pyroxene-plagioclase-quartz assemblages according to PERKINS and NEWTON (1981).

At the second stage average P-T calculations have been made using an updated version of the internally consistent thermodynamic dataset (HOLLAND and POWELL, 1990, 1998) and the program THERMOCALC (POWELL and HOLLAND, 1988). The results are shown in table 4 and plotted in figure 7a.

The independent set of end-member reactions for the assemblage garnet-clinopyroxene-plagioclase-quartz in mafic granulites, plagioclase-bearing retrograded eclogites and garnet clinopyroxenites used for average PT-estimates, includes four possible equilibria. For the amphibole-bearing garnet websterite the independent set of reactions includes seven equilibria for the paragenesis orthopyroxene-clinopyroxene-garnet-amphibole. As mentioned above for the kyanite eclogite, sodic plagioclase and zoisite are in textural equilibrium with omphacite, taramite and garnet. Nevertheless, the formation of these minerals at the later stage of retrogression cannot be excluded. For this reason average PT-estimates have been made for two mineral assemblages: garnet-omphacite-taramite-kyanite-paragonite-quartz, and the same minerals plus plagioclase and zoisite. In the first case the independent set of end-member reactions includes seven mineral equilibria and ten for the second one. The most important calculated reaction curves are shown in figure 7. Both average P-T estimates are near the reaction curve paragonite = jadeite + kyanite + H_2O. The average P-T values for the plagioclase-bearing association are very close to the interception of the calculated reaction curves paragonite = jadeite + kyanite + H_2O and jadeite + quartz = albite; they look quite reasonable at least for the late stage of high-pressure metamorphism. The higher P and lower T estimates for the plagioclase-free mineral assemblage may be unreasonable, but the alternative of simultaneous pressure decrease and temperature increase from early to late stage may also be assumed. On figure 7b we show two possible P-T-t trajectories for the early stage of the metamorphic evolution.

In general, both methods of P-T estimation give comparable results. Using the geothermometer of ELLIS and GREEN (1979) and the geobarometer of PERKINS and NEWTON (1981) yields

Tab. 4 P-T estimates for eclogite and associated mafic granulites of the Ubende belt.

No	Rock	Area	Mineral assemblage used in calculations	T °C	P kbar	σfit
TZS I	Ky-ecl	Tkola	Grt + Omph + Amf + Ky + Pl + Zo + Par + Qtz	724 ± 13	17.1 + 0.7	1.28
			Grt + Omph + Amf + Ky + Par + Qtz	609 + 66	19.7 + 1.5	1.53
S-1	R-ecl	Ikola	Grt + Cpx + Opx + Qtz	764 + 94	11.2 + 1.6	0.84
Sk35h	R-ecl	Ikola	Grt + Cpx + Pl + Qtz	620 + 77	10.2 + 1.3	0.67
Sk37b	R-ecl	Ikola	Grt + Cpx + Pl + Qtz	633 + 70	9.8 + 1.0	0.32
Sk37d	R-ecl	Ikola	Grt + Cpx + Pl + Qtz	763 + 92	11.2 + 1.4	1.33
Sk54f c	MG	Ikola	Grt + Cpx + Pl + Qtz	655 + 85	10.7 + 1.4	0.79
Sk54f r	MG	Ikola	Glt + Cpx + Pl + Qtz	579 + 73	9.0 + 1.2	0.09
Sk54k	MG	Ikola	Grt + Cpx + Pl + Qtz	637 + 79	9.3 + 1.2	0.51
Sk74b c	MG	Ikola	Grt + Cpx + Pl + Qtz	665 + 78	9.8 + 1.3	0.27
Sk74b r	MG	Ikola	Grt + Cpx + Pl + Qtz	652 + 75	9.7 + 1.3	0.15
279a2	R-ecl	Chisi	Grt + Cpx + Pl + Qtz	772 + 90	15.1 + 1.6	1.02
Sk82h	R-ecl	Chisi	Grt + Cpx + Pl + Qtz	684 + 90	13.4 + 2.0	0.57
Sk82k	R-ecl	Chisi	Grt + Cpx + Pl + Qtz	731 + 83	13.8 + 1.5	0.90
Sk8f	Grt-wb	Kungwe	Grt + Cpx + Opx + Amf	911 + 76	16.0 + 2.4	1.10
Sk9c c	MG	Kungwe	Grt + Cpx + Pl + Qtz	757 + 82	13.2 + 1.0	0.44
Sk9c r	MG	Kungwe	Grt + Cpx + Pl + Qtz	687 + 89	11.8 + 1.1	0.54
Sk10a c	MG	Kungwe	Grt + Cpx + Pl + Qtz	742 + 82	13.1 + 1.4	0.26
Sk10a r	MG	Kungwe	Grt + Cpx + Pl + Qtz	690 + 78	11.9 + 1.3	0.25
Sk10b c	MG	Kungwe	Grt + Cpx + Pl + Qtz	714 + 77	12.3 + 1.2	0.53
Sk10b r	MG	Kungwe	Grt + Cpx + Pl + Qtz	676 + 110	11.4 + 1.8	1.61
Sk10d	MG	Kungwe	Grt + Cpx + Pl + Qtz	699 + 74	12.4 + 1.3	0.46
Sk11c	MG	Kungwe	Grt + Cpx + Pl + Qtz	650 + 79	11.5 + 1.4	0.68
Sk449c	MG	Kungwe	Grt + Cpx + Pl + Qtz	693 + 84	12.6 + 1.0	0.78
Sk461 c	MG	Kungwe	Grt + Cpx + Pl + Qtz	677 + 69	12.1 + 1.3	0.96

Notes: abbreviation as in tables 1–5. P-T estimates from THERMICALC with 2σ errors of POWELL and HOLLAND (1988) and HOLLAND and POWELL (1990, 1998).

temperatures 30–100 °C higher and pressures 0.5–1 kbar lower as compared to the calculations of mineral reactions after HOLLAND and POWELL (1990, 1998).

Discussion

The eclogites described in this study show many features (intense overprinting, omphacite breakdown textures, etc.) common to eclogites of other areas as for example the Scandinavian Caledonides (e.g. AUSTRHEIM, 1990; KROGH et al., 1990; KROGH and CARSWELL, 1995). But the degree of high-temperature overprint is very high in the studied area. This caused complete re-equilibration of primary mineral assemblages. Only one pod of not retrograded kyanite eclogite and a few bodies of retrograded eclogites were found. Other garnet-rich rocks embedded in amphibolites are garnet pyroxenites and high-P granulites.

The garnet pyroxenites may be subdivided into two varieties: (i) true pyroxenites (former pyroxenites), for which high Mg/Mg + Fe ratio and high Cr-content are typical, refleced by compositions of rock-forming minerals (e.g. sample n24b) and completely retrograded eclogites (former gabbro or basalts). The latter are similar in textures, mineral assemblage and chemistry to retrograded eclogites except for the absence of omphacite relics and omphacite breakdown textures. P-T conditions for metamorphism for the true pyroxenites are likely to have been the same as for eclogites, but the presence of Na-augite instead of omphacite is explained by a bulk composition poor in Na.

Eclogites and garnet pyroxenites of the Ubende belt are the constituents of the basic-ultrabasic sequence that underwent a complex tectonometamorphic evolution. The results of this study, in combination with data on mafic granulites which are regarded as products of complete

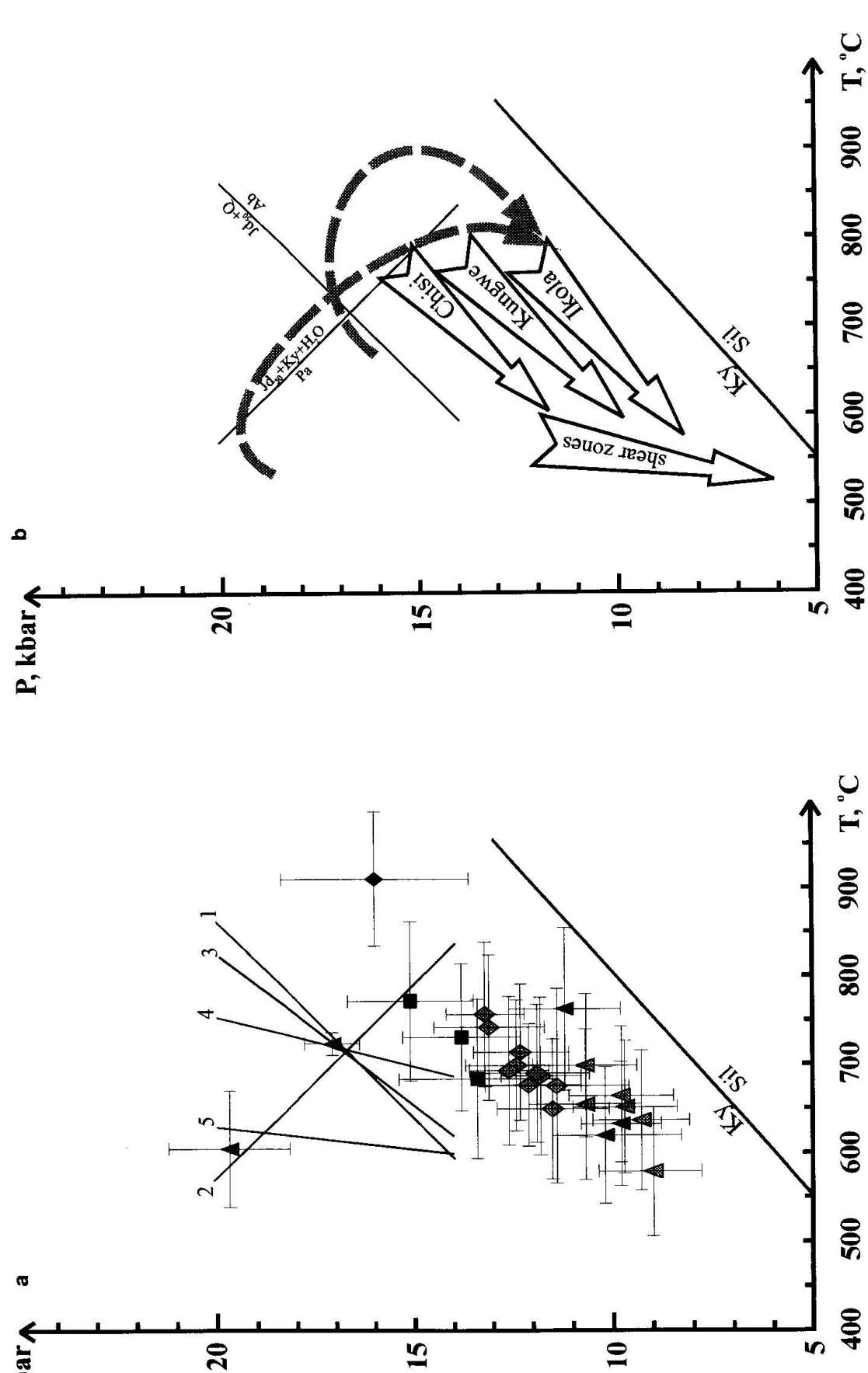

Fig. 7 P-T estimates with 2σ errors (a) and possible P-T paths (b) for investigated metamorphic rocks of the Ubende belt. P-T estimates of eclogites, retrograded eclogites, garnet pyroxenites (filled symbols), and associated mafic granulites (shadowed symbols) from the Ikola (triangles), Chisi (squares) and Kungwe bay (rhombs) areas are shown. Selected reaction curves for kyanite eclogite (TZS-1): (1) Jd + Qtz = Ab; (2) Par = Jd + Ky + H_2O; (3) Qtz + 2 Zo + Ky = 4 An + H_2O; (4) Qtz + Par = Ab + Ky + H_2O; (5) Py + 3 Hed = Alm + 3 Di. On the figure b proposed P-T paths of the early (shadowed dashed lines, two possible variants), second and late retrogression stages are shown. All average P-T estimates and reaction curves were calculated by the THERMOCALC program of Powell and Holland (1988) with the improved database of Holland and Powell (1990, 1998). In samples TZS-1 and Sk8f reactions were calculated for a_{H_2O} = 1. Aluminum silicate triple point after Salje (19986). For further explanation see text.

retrogression of eclogites in granulite-facies conditions (SKLYAROV et al., in prep.) and structural investigations (THEUNISSEN et al., 1996) suggest the following evolution scenario:

(1) Plate convergence and subduction of the oceanic slab under the Tanzanian craton. Strong obliteration of primary magmatic features makes the nature of the basic sequence (basalts, dykes or gabbro) somewhat uncertain and the side by side occurrence of different kinds of rocks in separate segments makes the complete reconstruction of the sequence difficult. Nevertheless the mafic and ultramafic sequences with associated metasedimentary rocks are regarded as an ophiolite suite. Alternating metaperidotite, pyroxenite and metagabbro in some segments and the common association banded granulite (metabasalt) with quartzites (metacherts) indeed suggest the ophiolite nature. The kyanite eclogite assemblages (T = 720 °C, P = 17.1 kbar) reflect the early metamorphic event during subduction (Fig. 7).

(2) Exhumation stage 1, recorded in retrograded eclogites (opx-cpx corona around garnet, breakdown of omphacite). The final P-T conditions of this stage (T = 800–850 °C, P = 11–15 kbar) are assumed as "initial" ones for mafic granulites (completely overprinted eclogites). Two types of eclogites are distinguished according to their mode of occurrence: (i) as constituents of essentially basic but dismembered tectonic units, known as the Ubende and Ikulu series and (ii) as rare small lenses in felsic gneiss. This distinction is considered as result of different exhumation mechanisms of the subducted plate. In the first case the relatively large slabs of essentially basic composition were uplifted from depth. In the second case former eclogites were exhumed to an intermediate level of the crust as xenoliths in ascending granitic magma. Afterwards this suite was involved in orogenic deformational processes. As the precise PT conditions for the peak temperature are uncertain, the shape of the metamorphic path between the prograde and the early exhumation part of the PT trajectory remains poorly defined and we assume two possibilities (Fig. 7b). Both include simultaneous heating and decompression at the beginning followed by decompression and cooling, but the shape of the P-T-t trajectories is different. Forced flow (ENGLAND and HOLLAND, 1979; CLOOS, 1982) is assumed to contribute to the early stage of uplift with a steep P/T gradient in to the 40–50 km level. Variations in the "initial" granulite P-T conditions (Fig. 7), as recorded in different areas, are tentatively interpreted as result of fragmentation and exhumation of slices of the subducted plate on different levels.

(3) Exhumation stage 2, reconstructed from the P-T evolution of mafic granulites and retrograded eclogites. This stage is characterised by more gentle P/T gradients (about 25 bar/°C). Subparallel trends of P-T evolution of different blocks can be explained by similar rates of uplift experienced or – in other words – by uplift of the whole pile, built up during a previous tectonic stage. So, initial and final PT conditions of metamorphism of the Chisi area refer to a lower, those of the Kungwe area to an intermediate, and those of the Ikola block to an upper level of this stacked pile. Lower P/T gradients may be explained either by lower rates of uplift (erosion or erosion combined with tectonic denudation of the upper crust) or by a higher T gradient during orogenesis.

(4) The final stage of exhumation is recorded in numerous shear zones, separating blocks and slices of mafic granulites, amphibolites (retrograded granulites) and associated metasedimentary rocks. Estimated temperatures are around 500–600 °C, and the pressure ranges between 5–10 kbar, reflecting a near-isothermal decompression trend (SKLYAROV et al., in prep.). This stage is likely to be responsible for the final juxtaposition of blocks with differing tectonometamorphic history, as observed in the present geological structure.

The ages of eclogite- and granulite facies metamorphism in the Ubende belt are unresolved, but available geochronological data (LENOIR et al., 1994; BOVEN et al., 1996) ensure that no major orogenic events took place in the Ubende belt after 1720–1740 Ma. According to PINNA (1995) the belt persists as an oblique suture, structurally frequently reactivated as a zone of horizontal stress transfer but never reworked by high grade metamorphism after Early Proterozoic. The repeated reactivation in the Proterozoic as well as in the Phanerozoic concentrated along and was confined to the inter-terrane boundaries, emplaced in the second phase paleo-Proterozoic evolution of the belt. Reactivation characteristically occurred in retrograde, generally greenschist facies conditions (THEUNISSEN et al., 1996). The described eclogites are probably synchronous with eclogites of the Usagara belt for which 2 Ga age is established (MÖLLER et al., 1995). If it is really so, the basite-ultrabasite sequences (dismembered ophiolites) and also the high-pressure metamorphism of eclogites and garnet pyroxenites are the petrological indicators of the earliest stages of plate tectonic evolution documented in Africa. We are aware that additional dating and petrological investigations of the basic-ultrabasic sequence are necessary for an unambiguous

reconstruction of the tectonometamorphic evolution of the Ubende belt. Such a work is now in progress and will be published later.

Acknowledgements

The paper summarizes research currently carried out by the Royal Museum of Central Africa (Belgium) in collaboration with the Institute of the Earth's Crust RAS (Russia) and in cooperation with the University of Dar es Salaam (Tanzania), with financial support of the Belgian Government, of INTAS (grant 93-134) and of the Russian Fundamental Science Foundation (grants 96-05-66290 and 96-05-64012). Drs. N. Karmanov and S. Kanakin are acknowledged for their appreciated assistance in microprobe analyses. Prof. L. Andre is acknowledged for his appreciated assistance in petrographic studies. Reviews by P.J. O'Brien and J. Ridley considerably improved the manuscript.

References

AUSTRHEIM, H. (1990): The granulite-eclogite facies transition: a comparison of experimental work and natural occurrence in the Bergen Arcs, Western Norway. In: OKRUSCH, M. (ed.): Third Int. Eclogite Conf. Spec. Issue. Lithos, 25, 163–169.

BOVEN, A., THEUNISSEN, K., SKLYAROV, E., KLERKX, J., MELNIKOV, A. and MRUMA, A. (submitted): Timing of exhumation of high-pressure mafic granulite terranes of the Paleoproterozoic Ubende Belt (West Tanzania). Precambrian Res.

CABY, R. (1994): Precambrian coesite from northern Mali: first record and implications for plate tectonics in the trans-Saharian segment of the Pan-African belt. Eur. J. Mineral., 6, 235–244.

CHOPIN, C. and SOBOLEV, N.V. (1995): Principal mineralogic indicators of UHP in crustal rocks. In: COLEMAN, R.G. and WANG, X. (eds): Ultrahigh pressure metamorphism. Cambridge University Press, New York, 96–131.

CLOOS, M. (1982): Flow melange: Numerical modelling and geologic constraints on their origin in the Franciscan subduction complex, California. Geol. Soc. Amer. Bull., 93, 330–345.

COOLEN, J.J.M. (1980): Chemical petrology of the Furua granulite complex, southern Tanzania. GUA, Amsterdam. Paper 13, 1–258.

COSI, M., DE BONIS, A., GOSSO, G., HUNZIKER, J., MARTINOTTI, G., MORATTO, S., ROBERT, J.P. and RUHLMAN, F. (1992): Late Proterozoic thrust tectonics, high-pressure metamorphism and uranium mineralization in the Domes Area, Lufilian Arc, northwestern Zambia. Precambrian Res., 58, 215–240.

DALY, M.C. (1988): Crustal shear zones in Central Africa: A kinematic approach to Proterozoic tectonics. Episodes, 11, 5–11.

DALY, M.C. and UNRIG, R. (1982): The Muva Supergroup of northern Zambia: a craton to mobile belt sedimentary sequence. Trans. Geol. Soc. South Africa, 85 (3), 155–165.

DALY, M.C., CHOROWICKS, J. and FAIRHEAD, J.D. (1989): Rift basin evolution in Africa: the influence of reactivated steep basement shear zones. In: COOPER, M.A. and WILLIAMS, G.D. (eds): Inversion tectonics. Geol. Soc. Spec. Publ., 44, 309–304.

DROOP, G.T.B. (1987): A general equation for estimating Fe^{3+} concentrations in ferromagnesian silicates and oxides from microprobe analyses, using stoichiometric criteria. Mineral. Mag., 51, 431–435.

ECKERT, J.O., NEWTON, R.C. and KLEPPA, O.J. (1991): The ΔH of reaction and recalibration of garnet-pyroxene-plagioclase-quartz geobarometers in the CMAS system by solution calorimetry. Amer. Mineralogist, 76, 148–160.

ELLIS, D.J. and GREEN, D.H. (1979): An experimental study of the effect of Ca upon garnet-clinopyroxene Fe–Mg exchange equilibria. Contr. Mineral. Petrol., 71, 13–22.

ENGLAND, P.C. and HOLLAND, T.J.B. (1978): Archimedes and the Tauern eclogites: the role of buoyancy in the preservation of exotic eclogite blocks. Earth and Planetary Sci. Let., 44, 287–294.

HACKER, B.R. and PEACOCK S.M. (1995): Creation, preservation and exhumation of UHPM rocks. In: COLEMAN, R.G. and WANG, X. (eds): Ultrahigh pressure metamorphism. Cambridge University Press, New York, 159–181.

HEPWORTH, J.V. (1972): Charnockitic granulites of some African cratons. Proc. 24th International Geological Congress, Montreal, Sect. 1, 126–134.

HOLLAND, T.J.B. (1979): Experimental determination of the reaction paragonite = jadeite + kyanite + H_2O, and internally consistent thermodynamic data for part of the system Na_2O–Al_2O_3–Si_2O–H_2O, with application to eclogites and blueschists. Contr. Mineral. Petrol., 68, 293–301.

HOLLAND, T.J. (1980): The reaction albite = jadeite + quartz determined experimentally in the range 600–1200 °C. Amer. Mineralogist, 65, 129–134.

HOLLAND, T.J. and POWELL, R. (1990): An enlarged and updated internally consistent thermodynamic dataset with uncertainties and correlations: the system K_2O–Na_2O–CaO–MgO–MnO–FeO–Fe_2O_3–TiO_2– SiO_2–C–H_2O. J. Metam. Geol. 8, 98–124.

HOLLAND, T.J. and POWELL, R. (1998): An internally consistent thermodynamic dataset for phases of petrological interest. J. Metam. Geol. in press.

KROGH, E.J., ANDERSEN, A., BRYHNI, I., BROKS, T.M. and KRISTENSEN, S.E. (1990): Eclogites and polyphase P-T cycling in the Caledonian Uppermost Allochthon in Troms, northern Norway. J. Metam. Geol., 8 (3), 289–309.

KROGH, E.J. and CARSWELL, D.A. (1995): HP and UHP eclogites and garnet peridotites in the Scandinavian Caledonides. In: COLEMAN, R.G. and WANG, X. (eds): Ultrahigh pressure metamorphism. Cambridge University Press, New York, 1244–1298.

LENOIR, J.L., LIEGEOIS, THEUNISSEN, K. and KLERKX, J. (1994): The Paleoproterozoic Ubendian shear belt in Tanzania: geochronology and structure. J. African Earth Sci., 19, 169–184.

MÉNOT, R.-P. and SEDDOH, K.F. (1984): The eclogites of the Lato hills, southern Togo, West Africa: Relics from the early tectonometamorphic evolution of the Pan-African orogeny. In: SMITH, D.C., FRANZ, G. and GEBAUER, D. (eds): Chemistry and Petrology of Eclogites. Chem. Geol., 50, 313–330.

MOLLER, A., APPEL, P., MEZGER, K. and SCHENK, V. (1995): Evidence for a 2 Ga subduction zone: Eclogites in the Usagaran belt of Tanzania. Geology, 23, 1067–1070.

PErkins, D. III. and NEWTON, R.C. (1981): Charnockite geobarometers based on coexisting garnet-pyroxene-plagioclase-quartz. Nature, 292, 144–146.

PINNA, P. (1995): On the dual nature of the Mozambique Belt, Mozambique to Kenya. J. African Earth Sciences, 21, 477–480.

POWELL, R. and HOLLAND, T.J.B. (1988): An internally consistent dataset with uncertainties and correlations: 3. Applications to geobarometry, worked examples and a computer program. J. Metam. Geol., 6, 173–204.

PRIEM, H.N.A., BOELRIJK, N.A.I.M., HEBEDS, E.H., VERDURMEN, E.A.TH. and VERSCHURE, R.H. (1979): Isotopic age determination on granitic and gneissic rocks from Ubendian-Usagarian System in southern Tanzania. Precambrian Res., 9, 227–239.

SALJE, E. (1986): Heat capacities and entropies of andalusite and sillimanite: the influence of fibrolitization on the phase diagram of the Al_2SiO_5. Amer. Mineralogist, 71, 1366–1371.

SANDERS, I.S., DALY, J.S. and DAVIES G.R. (1987): Late Proterozoic high pressure granulite facies metamorphism in the north-east Ox inlier, north-west Ireland. J. Metam. Geol., 5, 69–85.

SHACKELTON, R.M. and RIES, A.C. (1984): The relation between regionally consistent stretching lineations and plate motions. J. Struct. geol., 5, 111–117.

SHERVAIS, J.W., TAYLOR, L.A., LUGMAIR, G.W., CLAYTON, R.N., MAYEDA, T.K. and KOROTEV, R.L. (1988): Early Proterozoic oceanic crust and the evolution of subcontinental mantle: Eclogites and related rocks from southern Africa. GSA Bull. 100, 411–423.

SKLYAROV, E.V., THEUNISSEN, K., MELNIKOV, A.I., KLERKX, J. and MRUMA, A. (in prep.): High-pressure metamorphism of the Paleoproterozoic Ubende belt (Tanzania).

SMIRNOV, V.V., PENTELNIKOV, V., TOLOCHKO, V., TRIFAN, M. and ZHUKOV, S. (1973): Geology and minerals of the central part of the western rift. Unpublished report on geological mapping. Mineral and Resource Division, Dodoma, Tanzania, 1–333.

THEUNISSEN, K., KLERKX, J., MELNIKOV, A. and MRUMA, A. (1996): Mechanism of inheritance of rift faulting in the western branch of the East African rift (Tanzania). Tectonics, 15, 776–790.

UNGARETTI, L., SMITH, D.C. and ROCCI G. (1981): Crystal-chemistry by X-ray structure refinement and electron microprobe analysis of a series of sodic-calcic to alkali-amphiboles from the Nubo eclogite pod, Norway. Bulletin de Mineralogie, 104, 400–412.

Manuscript received September 8, 1997; revision accepted March 3, 1998.